ILAR e-JOURNAL

An Ovine Model of Postinfarction Dilated Cardiomyopathy in Animals with Highly Variable Coronary Anatomy

Paola Locatelli, Fernanda D. Olea, Oscar Mendiz, Fabián Salmo, Lucía Fazzi, Anna Hnatiuk, Rubén Laguens, and Alberto Crottogini

Volume 52(e16-e21) — 2011

THE NATIONAL ACADEMIES
Advisers to the Nation on Science, Engineering, and Medicine

ILAR e-Journal is the online, periodic, peer-reviewed publication of the Institute for Laboratory Animal Research (ILAR), National Research Council, 500 Fifth Street NW, Washington, DC 20001; Tel: 202-334-2590; Fax: 202-334-1687; Email: ILARJ@nas.edu; URL: www.dels.nas.edu/ilar. Membership in the ILAR Associates Program includes four print issues of *ILAR Journal* per year. Subscribe online at www.ilarjournal.com/subscriptions1.html or contact ILAR for more information. Online access: Both *ILAR e-Journal* and *ILAR Journal* articles are available online; institutional members have immediate access to current issues, for nonsubscribers issues and articles are available free of charge after 6 months. Permissions: Permission to use or reprint text or figures is granted for educational or research purposes only. Please contact ilarj@nas.edu for more information. *ILAR e-Journal* ISSN 1930-6180.

An Ovine Model of Postinfarction Dilated Cardiomyopathy in Animals with Highly Variable Coronary Anatomy

Paola Locatelli, Fernanda D. Olea, Oscar Mendiz, Fabián Salmo, Lucía Fazzi, Anna Hnatiuk, Rubén Laguens, and Alberto Crottogini

Abstract

Studies on cardiac regeneration require large mammalian models of dilated cardiomyopathy (DCM) after acute myocardial infarction (AMI), and pig and sheep models are increasingly used in this field of preclinical research. Given the large interindividual variability in ovine left anterior descending artery (LAD) anatomy, protocols based on the coronary arteries to be ligated often lead to significant variation in infarct sizes and hence to heterogeneous results, ranging from no ventricular remodeling to acute, lethal left ventricular (LV) failure. We designed an ovine model of postinfarction DCM based on estimated infarct size rather than on a predetermined menu of coronary artery ligatures. In seven adult sheep we induced an anterolateral AMI of approximately 25% of the LV mass by ligating the branches of the LAD that, by visual inspection, would lead to such an infarct size. In 10 to 12 weeks, LV end-diastolic volume more than doubled and LV end-systolic volume almost tripled. LV ejection fraction decreased dramatically, as did LV percent fractional shortening and LV percent wall thickening. Infarct size (planimetry) was approximately 25% of the LV endocardial surface. We conclude that in sheep, an anterolateral AMI of approximately 25% of the LV mass—regardless of the coronary branches ligated to attain that infarct size—results in a model of postinfarction DCM that may prove useful in preclinical research on myocardial regeneration.

Key Words: acute myocardial infarction (AMI); dilated cardiomyopathy (DCM); left anterior descending artery (LAD); ligature; ovine model; sheep

Introduction

After acute myocardial infarction (AMI1), the remaining viable myocardium undergoes ventricular remodeling, which leads to dilated cardiomyopathy (DCM[1]) and heart failure (Sutton and Sharpe 2000; Tiyyagura and Pinney 2006). The increasing worldwide incidence and prevalence of coronary artery disease (Rosamond et al. 2007), and hence of AMI and chronic heart failure, has motivated the search for strategies to replace the missing cardiomyocytes with new ones. The two main approaches for cardiomyogenesis are the implantation of adult or embryonic stem cells in the heart (Segers and Lee 2008) and the transfer of genes coding for either proteins involved in the regulation of the cell cycle or promitogenic growth factors (Laguens and Crottogini 2009). For reliable extrapolation of preclinical results to humans, both approaches (and diverse combinations derived from them) require testing in large mammalian models of postinfarction DCM. Dogs, pigs, and sheep are the large mammals most widely used for such research (Dixon and Spinale 2009).

Reported ovine models of DCM are designed on the basis of the coronary vessels that must be ligated. Both Gorman and colleagues (1998) and Moainie and colleagues (2002) reported that ligature of the first two diagonal branches of the left anterior descending coronary artery (LAD[1]) infarcts approximately 24% of the left ventricular (LV[1]) mass, leading to significant ventricular dilatation in about 8 weeks. Kramer and colleagues (1993) showed that ligation of the LAD at approximately 40% along its course from apex to base and of the second diagonal branch at its origin induces an infarct spanning 26±4% (mean ± SD) of the LV mass and, in turn, generates LV remodeling.

But when we tried to reproduce these models in our sheep, we observed considerable interindividual variability in left coronary artery anatomy that prevented us from replicating these protocols. The number, length, and originating site of the LAD diagonal branches varied greatly and inconsistently. Likewise, the circumflex artery varied its distribution and dominance, significantly contributing to irrigation of the LV anterior wall in some cases and not at all in others. Figure 1 illustrates this heterogeneity.

We therefore had to change the terms to achieve the desired infarct size rather than adopt a preestablished protocol

Paola Locatelli, MD, is a doctoral fellow of the National Agency for Scientific and Technological Investigation (ANPCyT) and Fernanda Daniela Olea, PhD, is a postdoctoral fellow of the National Council for Scientific and Technological Investigations (CONICET), both at the Department of Physiology of the Favaloro University in Buenos Aires, Argentina. Oscar Mendiz, MD, chairs Interventional Cardiology and Fabián Salmo, MD, is a staff physician of the Department of Echocardiography, both at the Favaloro University Hospital in Buenos Aires. Lucía Fazzi, MSc, is a fellow in training in the Department of Pathology at the Favaloro University. Anna Hnatiuk is a medical student at the Favaloro University Medical School. Rubén Laguens, MD, PhD, chairs the Department of Pathology and Alberto Crottogini, MD, PhD, chairs the Department of Physiology, both at the Favaloro University.

Address correspondence and reprint requests to Dr. Alberto Crottogini, Favaloro University, Solís 453, 1078 Buenos Aires, Argentina or email crottogini@favaloro.edu.ar.

[1]Abbreviations used in this article: AMI, acute myocardial infarction; DCM, dilated cardiomyopathy; DWTh, diastolic wall thickness; EDV, end-diastolic volume; EF, ejection fraction; ESV, end-systolic volume; FS, fractional shortening; LAD, left anterior descending coronary artery; LV, left ventricle; SWTh, systolic wall thickness; WTh, wall thickening

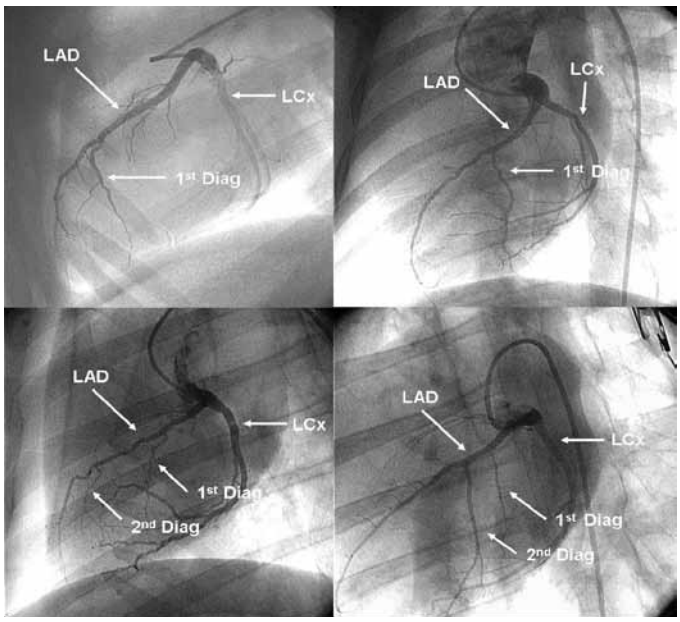

Figure 1 Left coronary artery angiograms from four Corriedale sheep in left anterior oblique projection. Significant interindividual variability is evident in the branching of the left anterior descending artery (LAD). The first and second diagonal branches (1st diag and 2nd diag) emerge from the LAD at diverse levels and exhibit inconsistent lengths and patterns of distribution. Similarly, the left circumflex artery (LCx) exhibits a heterogeneous distribution, contributing to very different extents to the irrigation of the left ventricular anterior wall.

of ligatures. In this article we show that it is possible to create a reproducible ovine model of postinfarct DCM by inducing an anterolateral infarct of approximately 25% of the LV mass based on the visual selection of the arteries that require ligation.

Methods

Surgical Preparation

We used seven adult male Corriedale sheep weighing 28 to 36 kg in procedures that complied with the *Guide for the Care and Use of Laboratory Animals* (NRC 2010) and were approved by the Favaloro University Laboratory Animal Care and Use Committee. After intramuscular (i.m.) premedication with acepromazine maleate (5 mg), anesthesia was induced with intravenous (i.v.) sodium thiopental (20 mg/kg) and maintained with 1.5% halothane in pure oxygen under mechanical ventilation (Neumovent, Córdoba, Argentina). To reduce the incidence of ventricular arrhythmias, we administered lidocaine (three bolus injections of 2 mg each and a 2 mg/kg infusion), amiodarone (150 mg infusion in 2 hours), and atenolol (2 mg).

We performed a sterile thoracotomy at the fourth intercostal space, opened the pericardium, and visually inspected the epicardial surface of the LV. Based on the distribution of the LAD and circumflex artery epicardial branches, we decided which vessel(s) required ligation to induce an anterolateral infarct of approximately 25% of the LV mass. We performed the ligatures sequentially using monofilament nylon; any subsequent ligatures were preceded by a brief occlusion of the selected vessels to see if the added ischemic zone contributed to achieve the desired infarct size. Finally, we repaired the thoracotomy and administered cephalotin (30 mg/kg, i.v.).

Echocardiography

Under sedation (diazepam, 10 mg, i.m.) and lying on its right lateral decubitus, each animal underwent transthoracic M-mode and bidimensional echocardiography (Sonos 1500, Hewlett Packard, Boston, MA) at preinfarction (baseline) condition and weekly thereafter until significant LV dilatation was observed. We measured LV end-diastolic volume (EDV[1]), LV end-systolic volume (ESV[1]), ejection fraction (%EF[1]), and fractional shortening (%FS[1]), and assessed end-systolic (SWTh[1]) and end-diastolic thickness of the anterior wall (DWTh[1]) as well as percent wall thickening (%WTh[1])[2] remote from the infarct.

Infarct Size Measurement

We opened the LV through an incision parallel to the posterior interventricular sulcus and laid it flat before fixation. We obtained digital photographs for image processing (Image-Pro Plus 4.1, Media Cybernetics, Silver Spring, MD) to determine LV and infarct areas. Infarct size was expressed as percent total LV endocardial area.

Histology

To compare the myocardial microscopic features of the model with those of normal sheep, we performed the following histological and morphometric cardiac analyses on the protocol sheep and on a comparison group of seven weight-, age-, and race-matched sheep from a study in which no heart interventions were performed. Hearts were fixed in 10% buffered formaldehyde and 5-μm-thick slices from paraffin-embedded normoperfused myocardial tissue were stained with hematoxylin-eosin. We measured cardiomyocyte diameter at the nuclear level in 200 cells using a digital analysis system (Image-Pro Plus 4.1) and determined percent collagen in 5-μm sections stained with Masson's trichrome.

Morphometry

A 1-mm-thick block from the noninfarcted area was cut into small pieces that were washed with distilled water and digested overnight in 12.5 M potassium hydroxide under mild agitation. After three washings, the tissue was vortexed and passed through a fine-tipped pipette 5 times; coarse tissue pieces were allowed to sediment. Isolated cardiomyocytes were collected from the supernatant and resuspended in 1% bovine serum

[2] We calculated %WTh as 100[(SWTh − DWTh)/DWTh].

albumin. To avoid shrinkage, cells were smeared on Vectabond-coated glass slides and dried under controlled humidity. Nuclei were stained with hematoxylin.

Cell length was calculated in 50 isolated cardiomyocytes with morphological integrity of the sarcolemma using digital analysis. Length data were adjusted to sarcomere length according to Gerdes and colleagues (1998). Assuming the cells are regular cylinders, cardiomyocyte volume (V) in μm^3 was calculated as $V = l (\mu r^2)$, where l is cell long axis length and r is half the diameter at the nuclear level.

Statistical Analysis

Using paired t-tests, we compared baseline and follow-up data. We then performed a t-test for unpaired data to compare dimensions of isolated cardiomyocyte from infarcted and noninfarcted sheep. Results are reported as mean ± SD; the level of statistical significance was set at $p < 0.05$.

Results

Infarct Size

Infarct size was 22.9±3.7% of the LV endocardial surface (Figure 2). We performed three ligatures in three sheep (43%), two ligatures in another three (43%), and one in the last sheep (14%) (Table 1 lists the ligatures performed in each animal). The most consistent ligature was that of the second diagonal branch (six sheep, 86%). The exception was an animal that exhibited only one large diagonal branch emerging from the middle third of the LAD. The second most consistent ligature was that of the third diagonal branch (five sheep, 71.4%), although not at its origin in two cases. The distal third of the

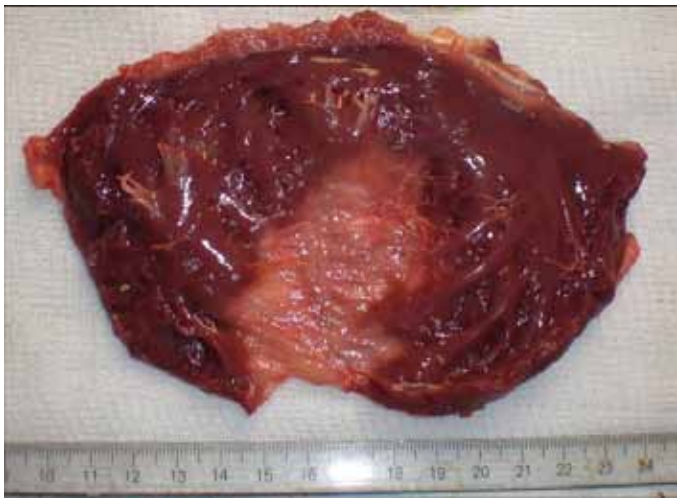

Figure 2 Endocardial view of the left ventricle of a Corriedale sheep 12 weeks after coronary artery occlusion. The ventricle has been opened along the posterior interventricular sulcus and laid flat. The sharply delimited pale area is the infarcted zone.

Table 1 Vessel(s) ligated in each individual animal

	Sheep number						
Ligated vessel	**1**	**2**	**3**	**4**	**5**	**6**	**7**
2nd diagonal branch of LAD	X	X	X	X	X	X	
3rd diagonal branch of LAD at origin	X		X		X		
3rd diagonal branch of LAD distal 1/3		X					
3rd diagonal branch of LAD distal 2/3						X	
1st diagonal branch of LAD	X						X
LAD distal 1/3				X			
Marginal obtuse of Cx distal 1/4					X		

Cx, circumflex artery; LAD, left anterior descending artery

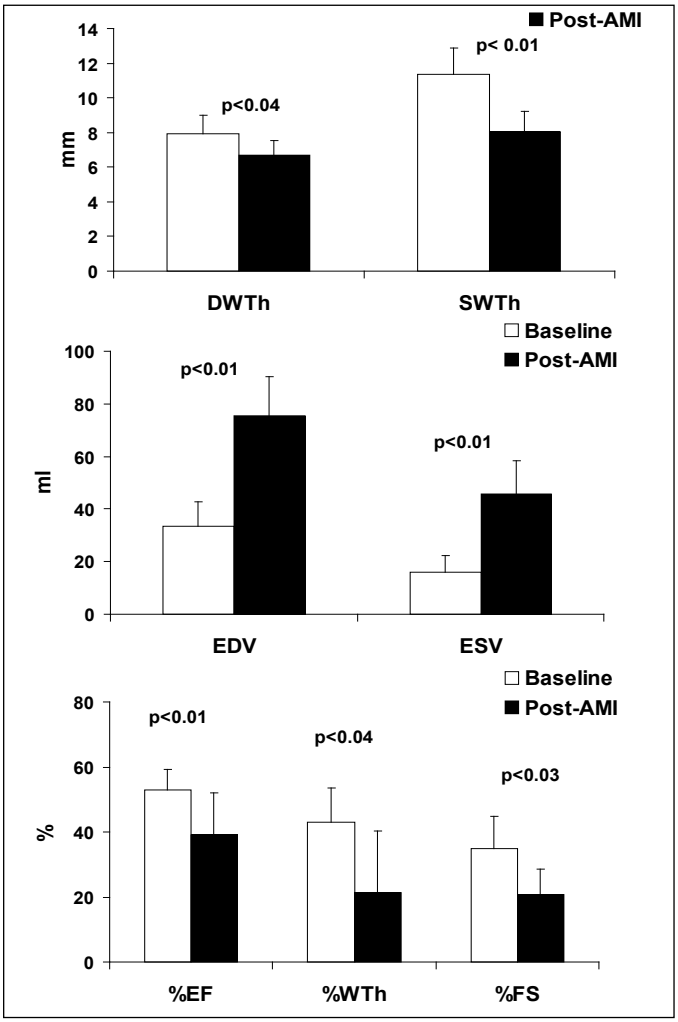

Figure 3 Echocardiographic measures of left ventricular function at baseline and at the end of the study. End-diastolic wall thickness (DWTh) decreased from 8±0.9 to 6.7±0.9 mm ($p < 0.04$) and end-systolic wall thickness (SWTh) from 11.4±1.5 to 8±1.2 mm ($p < 0.01$). End-diastolic volume (EDV) increased from 33.4±9.5 to 75.5±14.7 ml ($p < 0.01$) and end-systolic volume (ESV) from 16±6.4 to 45.9±12.4 ml ($p < 0.01$). Percent ejection fraction (%EF) decreased from 53±6.2 to 39.2±12.8% ($p < 0.01$), percent wall thickening (%WTh) from 43.1±10.4 to 21.5±19% ($p < 0.04$) and percent fractional shortening (%FS) from 34.8±9.9 to 20.9±7.7% ($p < 0.03$). AMI, acute myocardial infarction.

LAD and the first diagonal branch were ligated 2 times (28.6% each), and in one animal we ligated the distal, bifurcating portion of a large obtuse marginal branch of the left circumflex artery.

Echocardiography

Animals developed significant LV dilatation after 9.4±4.4 weeks of coronary occlusion (2 weeks: $n = 1$; 4 weeks: $n = 1$; 12 weeks: $n = 5$). As shown in Figure 3, EDV more than doubled and ESV almost tripled; LV %EF decreased significantly, as did %FS and %WTh. Figure 4 shows the short and long axis echocardiograms of one sheep at baseline and after 12 weeks of coronary occlusion.

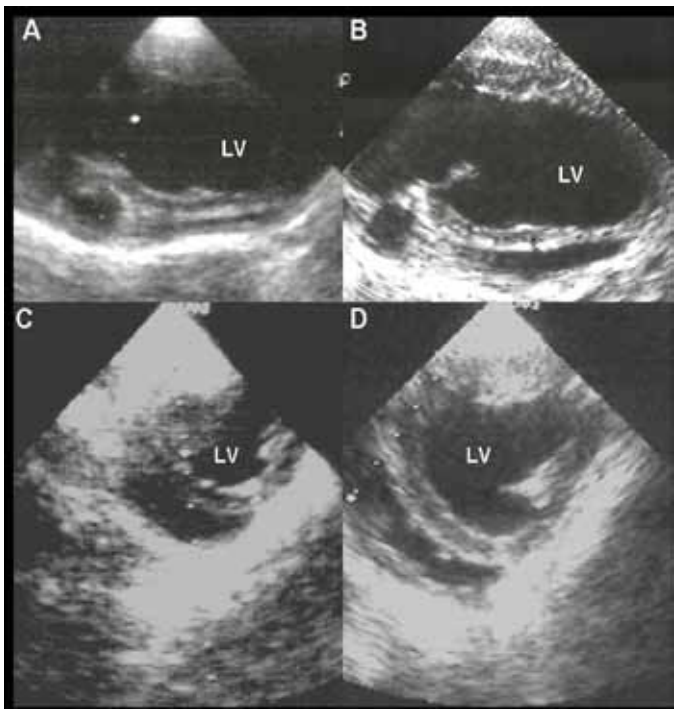

Figure 4 Long axis (A and B) and short axis (C and D) echocardiographic views of the left ventricle in one sheep. Significant chamber enlargement developed between baseline condition (A and C) and 12 weeks after myocardial infarction (B and D).

Histology and Morphometry

Cardiomyocyte length was smaller in infarcted sheep than in normal, noninfarcted weight-matched sheep (normal: 132±12 µm; infarcted: 113±13 µm, $p < 0.01$). However, there was no difference between infarcted and normal sheep in either the cardiomyocyte radius (normal: 7.74±0.33 µm, infarcted: 7.73±0.67 µm, p = not significant NS) or volume (normal: 25,009±3,011 µm, infarcted: 21,355±4,178 µm, p = NS).

Fibrosis was confined to the infarct scar; the myocardium distal to the infarct was free of fibrosis.

Discussion

Most preclinical research on heart regeneration is performed on mice and rats. Although there are similarities in structure, metabolic pathways, and physiology between the cardiomyocytes of humans and laboratory rodents, important interspecies differences (e.g., in heart size, time of gestation, and lifespan) suggest that, certainly in research concerning myocyte growth, replication, and regeneration capacity, direct extrapolation of rat and mice results to humans is risky. Therefore large mammalian models of diseases characterized by contractile cell loss are necessary.

One of the most important challenges in cardiomyogenesis research is halting or reversing the postinfarction ventricular remodeling process that leads to DCM and heart failure. Once heart failure has developed (and in the absence of a heart transplant), 1-year mortality is about 40% (Levy et al. 2002; McMurray and Pfeffer 2005; Stevenson 2005).

Given the direct relationship between initial infarct size and degree of remodeling (Lenderink et al. 1995; Pfeffer et al. 1991), large mammalian models of postinfarct dilated cardiomyopathy should be based on the desired extent of myocardial necrosis, especially for species with heterogeneous coronary anatomy. As discussed above, in such species the use of a predetermined protocol of vessels to be occluded may lead to extensive variation in final infarct size.

We aimed to produce an infarct comprising 20–25% of the LV anterolateral wall and determined what ligatures to perform based on visual inspection of the LV epicardial surface. Using this method, we induced a postinfarction remodeling process that led to significant LV dilatation and reduced LV wall motion and ejection fraction in a mean time of 10 weeks. While five out of seven animals developed DCM in 3 months, two did so in 2 and 4 weeks. We did not observe any histological differences that could explain this difference.

Despite significant chamber dilatation and decreased wall thickness, we did not observe certain ultrastructural characteristics of remodeling, namely cardiomyocyte hypertrophy and replacement of contractile cells by fibrotic tissue (Sutton and Sharpe 2000; Zornoff et al. 2009). This latter finding agrees with the results of Kramer and colleagues (1993), who observed that, in sheep with significant LV remodeling after 6 months of infarction, the myocardium more than 7 mm from the infarct border was free of fibrosis.

Findings similar to those of Kramer and colleagues were reported by Monreal and colleagues (2008) in sheep with heart failure induced by microembolization of the circumflex coronary artery. They observed that despite extensive LV remodeling and dilatation, fibrosis in the noninfarcted anterior wall up to 12 months after infarction was within normal range and comparable to the 2-4% fibrosis in healthy adult human myocardium (Brower et. al 2006). Only after 1 year did fibrosis appear in their sheep. With regard to cardiomyocyte hypertrophy, after 4 months of heart failure there were no statistically significant differences in myocyte size as compared to baseline. Furthermore, their findings reveal a tendency for myocytes to

be smaller at 4 months than at baseline (Monreal et al. 2008, figure 2), a result similar to ours.

Monreal and colleagues (2008) concluded that fibrosis and myocyte hypertrophy are temporally and spatially heterogeneous in heart failure and that, although these features are standard markers for heart failure, myocytes themselves undergo an "intracellular remodeling" associated with both excess desmin expression and changes in other cytoskeletal proteins (Schaper et al. 1991). This intracellular remodeling induces an alteration in myocyte mechanical properties and this alteration is the inciting mechanism for physiological abnormalities and LV dysfunction.[3]

The paucity of ultrastructural changes in our sheep was consistent with the modest degree of LV functional decline in relation to the change in chamber dimensions: while LV volumes more than doubled, ejection fraction decreased by roughly 25%. Our model thus induces clinical DCM with only mild to moderate heart failure and may thus represent an advantage for studying gene transfer or stem cell–mediated therapies to alleviate or reverse remodeling. In contrast, severely damaged myocardial tissue may hardly respond to any intervention, thus obscuring its potential usefulness.

Finally, it is important to bear in mind that comparison of sheep and human models includes variables other than coronary anatomy. Concerning contractile proteins, the predominance of myosin heavy chain isoform expression and combination in different regions of the heart varies among species (Schiaffino and Reggiani 1996) as does the apparent molecular mass of fast-type myosin light chain. Because these variations correlate with species body size (Bicer and Reiser 2007), adult sheep may be reasonably comparable to humans in this regard. Metabolic pathways involved in ischemia-reperfusion injury should also be considered. Xanthine oxidase, which plays a major role as a source of reactive oxygen species in such injury, is consistently present in ovine heart tissue (Al-Khalidi and Chaglassian 1965; DeWall et al. 1971), but there is controversy about its presence in human myocardium, with reports showing its absence (Downey et al. 1988; Linder et al. 1999; Tavenier et al. 1995), minimal expression (de Jong et al. 1990; Moriwaki et al. 1993), and significant presence (Hellsten-Westing 1993).

Conclusion

In cardiac regeneration research (as in other biomedical investigations), it is appropriate to test novel therapies on large mammalian models before moving forward to clinical trials. For postinfarction dilated cardiomyopathy, the most prevalent of the diseases characterized by myocardial cell loss, ovine models are advantageous because of the similarity between sheep and human cardiomyocytes. Infarct size is crucial for the development of DCM and ventricular remodeling. While protocols preestablishing the vessel(s) to be ligated may result in consistent infarct sizes in species with constant, repeatable coronary anatomy and distribution, they fail in species that exhibit large interindividual variability in coronary anatomy. In these cases, a preestablished desired infarct size should be the guideline, tailored to the coronary distribution of each animal.

We showed that, in adult Corriedale sheep, an anterolateral myocardial infarction of approximately 25% of the LV mass—regardless of the coronary branches ligated to attain that infarct size—results in a model of postinfarction DCM that may prove useful in preclinical research on myocardial regeneration.

[3]In humans, myocyte diameter increases significantly in diastolic but not systolic heart failure (20.3±0.6 µm for the former and 15.1±0.4 µm for the latter; van Heerebeek et al. 2006).

Acknowledgments

We thank Julio Martínez and Fabián Gauna for technical help. We are also grateful to veterinarians María Inés Besansón, Pedro Iguain, and Marta Tealdo, and veterinary assistants Juan Ocampo, Osvaldo Sosa, and Juan Carlos Mansilla for dedicated animal care. Supported by grant PAE-PICT 069 from the National Agency for Scientific and Technological Promotion (ANPCyT) of Argentina.

References

Al-Khalidi UA, Chaglassian TH. 1965. The species distribution of xanthine oxidase. Biochem J 97:318-320.

Bicer S, Reiser PJ. 2007. Variations in apparent mass of mammalian fast-type myosin light chains correlate with species body size, from shrew to elephant. Am J Physiol Regul Integr Comp Physiol 292:R527-R534.

Brower G, Gardner J, Forman M, Murray D, Voloshenyuk T, Levick S. 2006. The relationship between myocardial extracellular matrix remodeling and ventricular function (review). Eur J Cardiothorac Surg 30:604-610.

de Jong JW, van der Meer P, Nieukoop AS, Huizer T, Stroeve RJ, Bos E. 1990. Xanthine oxidoreductase activity in perfused hearts of various species, including humans. Circ Res 67:770-773.

DeWall RA, Vasko KA, Stanley EL, Kezdi P. 1971. Responses of the ischemic myocardium to allopurinol. Am Heart J 82:362-370.

Dixon JA, Spinale FG. 2009. Large animal models of heart failure: A critical link in the translation of basic science to clinical practice. Circ Heart Fail 2:262-271.

Downey JM, Hearse DJ, Yellon DM. 1988. The role of xanthine oxidase during myocardial ischemia in several species including man. J Mol Cell Cardiol 20(Suppl 2):55-63.

Gerdes AM, Onodera T, Tamura T, Said S, Bohlmeyer TJ, Abraham WT, Bristow MR. 1998. New method to evaluate myocyte remodeling from formalin-fixed biopsy and autopsy material. J Card Fail 4:343-348.

Gorman JH 3rd, Gorman RC, Plappert T, Jackson BM, Hiramatsu Y, St John-Sutton MG, Edmunds LH Jr. 1998. Infarct size and location determine development of mitral regurgitation in the sheep model. J Thorac Cardiovasc Surg 115:615-622.

Hellsten-Westing Y. 1993. Immunohistochemical localization of xanthine oxidase in human cardiac and skeletal muscle. Histochemistry 100:215-222.

Kramer CM, Lima JA, Reichek N, Ferrari VA, Llaneras MR, Palmon LC, Yeh IT, Tallant B, Axel L. 1993. Regional differences in function within noninfarcted myocardium during left ventricular remodeling. Circulation 88:1279-1288.

Laguens RP, Crottogini AJ. 2009. Cardiac regeneration: The gene therapy approach. Expert Opin Biol Ther 9:411-425.

Lenderink T, Simoons ML, Van Es GA, Van de Werf F, Verstraete M, Arnold AE. 1995. Benefit of thrombolytic therapy is sustained throughout five years and is related to TIMI perfusion grade 3 but not grade 2 flow at discharge. The European Cooperative Study Group. Circulation 92:1110-1116.

Levy D, Kenchaiah S, Larson MG, Benjamin EJ, Kupka MJ, Ho KK, Murabito JM, Vasan RS. 2002. Long-term trends in the incidence of and survival with heart failure. N Engl J Med 347:1397-1402.

Linder N, Rapola J, Raivio KO. 1999. Cellular expression of xanthine oxidoreductase protein in normal human tissues. Lab Invest 79:967-974.

McMurray JJ, Pfeffer MA. 2005. Heart failure. Lancet 365:1877-1889.

Moainie SL, Gorman JH 3rd, Guy TS, Bowen FW 3rd, Jackson BM, Plappert T, Narula N, St John-Sutton MG, Narula J, Edmunds LH Jr, Gorman RC. 2002. An ovine model of postinfarction dilated cardiomyopathy. Ann Thorac Surg 74:753-760.

Monreal G, Nicholson LM, Han B, Joshi MS, Phillips AB, Wold LE, Bauer JA, Gerhardt MA. 2008. Cytoskeletal remodeling of desmin is a more accurate measure of cardiac dysfunction than fibrosis or myocyte hypertrophy. Life Sci 83:786-794.

Moriwaki Y, Yamamoto T, Suda M, Nasako Y, Takahashi S, Agbedana OE, Hada T, Higashino K. 1993. Purification and immunohistochemical tissue localization of human xanthine oxidase. Biochim Biophys Acta 1164:327-330.

NRC [National Research Council]. 2010. Guide for the Care and Use of Laboratory Animals, 8th ed. Washington: National Academies Press.

Pfeffer JM, Pfeffer MA, Fletcher PJ, Braunwald E. 1991. Progressive ventricular remodeling in rat with myocardial infarction. Am J Physiol Heart Circ Physiol 260:H1406-H1414.

Rosamond W, Flegal K, Friday G, Furie K, Go A, Greenlund K, Haase N, Ho M, Howard V, Kissela B, Kittner S, Lloyd-Jones D, McDermott M, Meigs J, Moy C, Nichol G, O'Donnell CJ, Roger V, Rumsfeld J, Sorlie P, Steinberger J, Thom T, Wasserthiel-Smoller S, Hong Y. 2007. Heart disease and stroke statistics—2007 update: A report from the American Heart Association Statistics Committee and Stroke Statistics Subcommittee. Circulation 115:e69-e171.

Schaper J, Froede R, Hein S, Buck A, Hashizume H, Speiser B, Friedl A, Bleese N. 1991. Impairment of the myocardial ultrastructure and changes of the cytoskeleton in dilated cardiomyopathy. Circulation 83:504-514.

Schiaffino S, Reggiani C. 1996. Molecular diversity of myofibrillar proteins: Gene regulation and functional significance. Physiol Rev 76:371-423.

Segers VF, Lee RT. 2008. Stem-cell therapy for cardiac disease. Nature 451:937-942.

Stevenson LW. 2005. Design of therapy for advanced heart failure. Eur J Heart Fail 7:323-331.

Sutton M, Sharpe N. 2000. Left ventricular remodeling after myocardial infarction: Pathophysiology and therapy. Circulation 101:2981-2988.

Tavenier M, Skladanowski AC, De Abreu RA, de Jong JW. 1995. Kinetics of adenylate metabolism in human and rat myocardium. Biochim Biophys Acta 1244:351-356.

Tiyyagura SR, Pinney SP. 2006. Left ventricular remodeling after myocardial infarction: past, present, and future. Mt Sinai J Med 73:840-851.

van Heerebeek L, Borbély A, Niessen HW, Bronzwaer JG, van der Velden J, Stienen GJ, Linke WA, Laarman GJ, Paulus WJ. 2006. Myocardial structure and function differ in systolic and diastolic heart failure. Circulation 113:1966-1973.

Zornoff L, Paiva S, Duarte D, Spadaro J. 2009. Ventricular remodeling after myocardial infarction: Concepts and clinical implications. Arq Bras Cardiol 92:150-164.